Dynamics of adatoms of the Si(111)-(7×7) surface studied by reflection high-energy positron diffraction

Y. Fukaya,* A. Kawasuso, K. Hayashi, and A. Ichimiya
Advanced Science Research Center, Japan Atomic Energy Research Institute, 1233, Watanuki, Takasaki, Gunma, 370-1292, Japan
(Received 18 May 2004; revised manuscript received 2 September 2004; published 17 December 2004)

The thermal vibrational amplitude of adatoms of 0.14 Å at 293 K and 0.23 Å at 873 K are determined at the total reflection scheme. The surface Debye temperature of 290 K is also determined from the temperature dependences of positron diffraction intensities which are measured in the temperature range of 273 to 873 K. From the analysis based on the dynamical diffraction theory and considering the thermal diffuse scattering, the average thermal vibrational amplitude of the surface atoms is enhanced as compared to that obtained in previous studies. This result indicates that the adatom bonds of the Si(111)-(7×7) surface become softer at temperatures considerably below the 7×7 to 1×1 phase transition temperature.

DOI: 10.1103/PhysRevB.70.245422 PACS number(s): 68.35.Rh, 68.35.Bs, 61.14.Hg

I. INTRODUCTION

In order to understand the processes of adsorption, phase transition, and so on, it is very important to study the dynamics of surface atoms, in particular the topmost surface atoms. The thermal vibrational amplitude of bulk atoms is accurately determined using the x-ray and neutron diffraction techniques.[1] Electron diffraction is generally used to determine the thermal vibrational amplitude of surface atoms. However, while using electrons, it is rather difficult to obtain such quantities without any influence of the bulk, because electrons penetrate several layers and the measured quantities are averaged over several layers from the surface.

Positron diffraction is a powerful tool in order to study the atomic structure and vibrational state associated with surfaces.[2–7] One great advantage of this method is the appearance of the total reflection of positrons on account of their positive charge.[2] On the other hand, total reflection never occurs in the case of electron diffraction. In the total reflection mode, the diffraction intensity is extremely sensitive to the first layer. Owing to this property, the atomic coordinates and the thermal vibrational amplitudes of the topmost surfaces can be determined using reflection high-energy positron diffraction (RHEPD). Recently, we succeeded in observing the RHEPD patterns of a Si(111)-(7×7) reconstructed surface.[8,9] We also reported the preliminary results of the surface Debye temperature of a Si(111)-(7×7) surface.[10] Although the basic structure of the Si(111)-(7×7) reconstructed surface has already been revealed as possessing a dimer-adatom-stacking fault layer (DAS),[11] it continues to be an interesting subject with respect to dynamics and phase transition, because of its complexity. Recently,[8] we observed that the adatom height is much greater than that predicted by theoretical calculations[12] and the electron diffraction analysis,[13–15] and slightly smaller than that predicted by the x-ray diffraction analysis.[16] More recent theoretical calculations showed a large distance between the adatoms and the underlying atoms.[17] The large shift in the adatom position toward the vacuum region might occur due to the soft bond, and hence, it may result in large vibrational amplitude.

In this study, we measured the temperature dependence of the RHEPD intensity of the Si(111)-(7×7) surface to investigate the thermal vibration of the adatoms. The RHEPD rocking curves were also carefully analyzed. We will demonstrate that the thermal vibrational amplitude of adatoms is sufficiently enhanced as compared with that determined in previous studies.

II. EXPERIMENTAL PROCEDURE

The samples used in this study were cut from a mirror-polished *n*-type Si(111) wafer with a resistivity of 1–10 Ω cm ($0.5\times0.1\times15$ mm^3). They were rinsed in ethanol and introduced into a UHV chamber. After degassing at 673 K for several hours, the samples were flashed at 1500 K for 10 s a few times by passing a direct current. Auger peaks due to the presence of contaminations such as O and C atoms were not detected. Through this experiment, clear 7×7 spots were confirmed through reflection high-energy electron diffraction (RHEED). The substrate temperature (T) was calibrated using an optical pyrometer.

The RHEPD experiments were carried out using a 20 keV positron beam generated with an electrostatic beam apparatus. The details have been described elsewhere.[6,18] The glancing angle (θ) and the azimuthal angle (φ) of the incoming positrons were mechanically adjusted by tilting and rotating the sample mounted to the manipulator. In this case, $\varphi=0°$ and $\varphi=90°$ corresponded to the $[11\bar{2}]$ and $[\bar{1}10]$ directions, respectively. The rocking curves were measured from $\theta=0.5°$ to 4.5° with steps of 0.1° at $\varphi=7.5°$. This azimuthal angle is called the one-beam condition, under which the specular beam is the most significant diffraction spot, because a simultaneous reflection in the surface-parallel direction is suppressed.[13] The temperature dependence of the RHEPD intensity was also measured under various conditions; the (00) spot intensities at (i) $\theta=1.0°$ and $\varphi=7.5°$, (ii) $\theta=1.6°$ and $\varphi=7.5°$, (iii) $\theta=3.5°$ and $\varphi=7.5°$, and the (11) spot intensity at (iv) $\theta=1.0°$ and $\varphi=1.5°$ were measured. Moreover, the (00) spot intensities at $\theta=1.0°$ and $\varphi=0.0°$ and at $\theta=1.0°$ and $\varphi=90.0°$ were measured.

III. RESULTS AND DISCUSSIONS

Figure 1 shows the RHEPD rocking curves of the (00) spot from the Si(111)-(7×7) surface measured at various

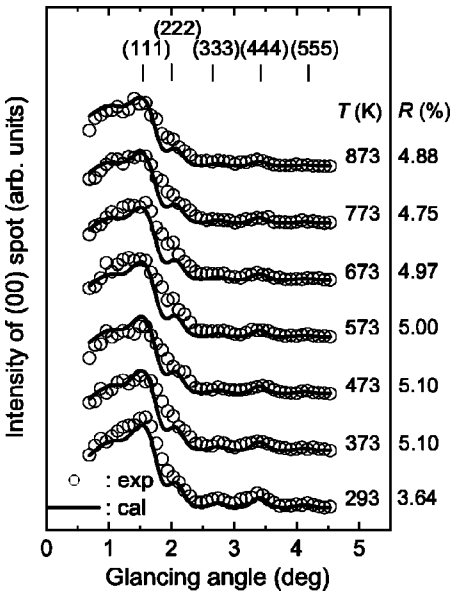

FIG. 1. RHEPD rocking curves from the Si(111)-(7×7) surface up to 873 K (open circles). Solid lines denote the intensities calculated using Θ_S=290 K and Θ_B=600 K (see text).

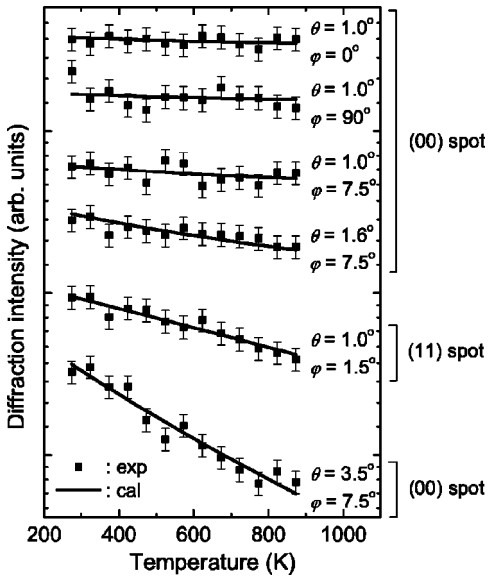

FIG. 2. Temperature dependences of the RHPED intensities from a Si(111)-(7×7) surface (closed squares). Solid lines represent the calculated intensities using Θ_S=290 K and Θ_B=600 K.

temperatures under the one-beam condition. In this case, the critical angle (θ_c) of the total reflection for positron can be expressed using the Snell's equation as

$$\theta_c = \arcsin\left(\frac{eV_0}{E}\right)^{1/2}, \tag{1}$$

where V_0 and E are the mean inner potential of Si (12 V) and the accelerating energy of the incident positron, respectively.[2] The RHEPD intensity is high in the total reflection region ($\theta_c < 1.4°$), as reported in previous studies.[8] The (111) Bragg peak of the rocking curve can be clearly identified. Similar to electron diffraction, (222), (333), (444), and (555) Bragg peaks appear over the critical angle. It should be noted that the (111) Bragg spot is observed in the positron diffraction. The (111) Bragg peak can never be observed in electron diffraction because of the refraction effect. At elevated temperatures, the rocking curve does not exhibit any significant change; that is, intensities of only the Bragg peaks decrease with increasing temperatures. However, the RHEPD intensity of the total reflection is not altered by the change in temperature. Detailed analyses of the rocking curves will be performed after determining the surface Debye temperature.

Figure 2 shows the temperature dependence of the intensities of the (00) spots and the (11) spot under various conditions. In this case, θ=1.0° satisfies the total reflection condition. Also, θ=1.6° and θ=3.5° satisfy the (111) and (444) Bragg conditions, respectively. The (00) spot intensities at θ=1.0° exhibit only a minor temperature dependence at any azimuthal angles; whereas the attenuation of the (11) spot intensity at θ=1.0° is greater than the (00) spot intensity. The slope of the (111) Bragg spot intensity can be compared with that of the (11) spot intensity. The diffracted intensity at the (444) Bragg reflection, which is outside the total reflection region, exhibits sufficient temperature dependence.

Positrons are decelerated in the crystal because the crystal potential is positive. On the other hand, the electrons are accelerated in the crystal. Thus, the wavelength of the positron beam in the crystal is larger than that in vacuum and hence the refractive index is less than unity. For positrons, the total reflection takes place below the critical angle obtained from Eq. (1).[2] At the small angles that result in the total reflection, the magnitude of the scattering vector for the (00) spot is nearly zero in the crystal. The Debye-Waller factor, $\exp(-Bs^2)$, where $B=8\pi^2\langle u^2\rangle$, **s** is the scattering vector, and $\langle u^2\rangle$ is the mean square amplitude of thermal vibration, is close to unity. Therefore, the (00) spot intensity in the total reflection region does not decrease strongly with increasing temperatures, irrespective to B. Although the glancing angle for the (11) spot satisfies the total reflection, the magnitude of the scattering vector parallel to the surface, and hence Bs^2, are finite. Therefore, relatively, the (11) spot intensity decreases strongly as compared with that of the (00) spot at θ=1.0°. The scattering vector of the (111) Bragg reflection is also nonzero. Therefore, the temperature dependence can be observed. Similarly, with temperature, more attenuation of the (444) Bragg reflection is observed. On the whole, the slope of the RHEPD intensity has a tendency to increase with the magnitude of the scattering vector. The Debye parameter B will be determined based on a comparison with the theoretical calculations as shown below.

The temperature dependence of the RHEPD intensity obtained in the preceding section can be reproduced by a numerical calculation based on the dynamical diffraction theory while considering the thermal diffuse scattering.[19] By taking into account the absorption due to inelastic scattering, the total crystal potential can be written as

$$V = V^{\text{elastic}} + iV^{\text{TDS}} + iV^{\text{el}}, \tag{2}$$

where V^{elastic} is obtained from the elastic scattering. V^{TDS} and V^{el} result from inelastic scattering occurring due to thermal

diffuse scattering and electronic excitation, respectively. As regards the elastic scattering, the Fourier component of the crystal potential is written as

$$V_g^{\text{elastic}} = \frac{\hbar^2}{2m_0}\frac{4\pi}{\Omega}\sum_i \exp(-i\mathbf{g}\cdot\mathbf{R}_i)f(s)\exp(-Bs^2), \quad (3)$$

where Ω and $\mathbf{R}_i$ are the unit cell volume and the atomic position, respectively, $\hbar$ is the Plank constant, m_0 is the electron rest mass, and $\mathbf{g}$ is the reciprocal lattice vector ($\mathbf{s}=\mathbf{g}/4\pi$).[20] In the Einstein approximation, $\langle u^2\rangle$ is obtained by

$$\langle u^2\rangle = \frac{\sqrt{3}\hbar^2}{k_B M_a \Theta}\left[\frac{1}{2}+\frac{1}{\exp(\Theta/\sqrt{3}T)-1}\right], \quad (4)$$

where Θ is the Debye temperature and M_a is the mass of Si atom.[21] Although the use of Eq. (4) is valid for the bulk, we assumed that the use of this equation is also valid for the surface.[22] $f(s)$ is the elastic scattering factor and is expressed as the form of the Gaussian sum

$$f(s) = \sum_n a_n \exp(-b_n s^2). \quad (5)$$

The Gaussian coefficients, a_n and b_n have been tabulated by Doyle and Turner[23] and Dudarev *et al.*[24] As regards thermal diffuse scattering, the Fourier component of the absorption potential is written in the same form as the elastic scattering

$$V_g^{\text{TDS}} = -\frac{\hbar^2}{2m_0}\frac{4\pi}{\Omega}\sum_i \exp(-i\mathbf{g}\cdot\mathbf{R}_i)f'(s)\exp(-Bs^2), \quad (6)$$

where $f'(s)$ is the absorptive scattering factor resulting from the thermal diffuse scattering

$$f'(s) = \frac{4\pi\hbar}{m_0 v}\int d^2s' f\left(\left|\frac{\mathbf{s}}{2}+\mathbf{s}'\right|\right) f\left(\left|\frac{\mathbf{s}}{2}-\mathbf{s}'\right|\right) \times\{1-\exp[-2B(s'^2-s^2/4)]\}, \quad (7)$$

where v is the velocity of the incident positrons and $\mathbf{s}'$ is the scattering vector.[20] Dudarev *et al.* represented it as a sum of the Gaussian terms, similar to the Doyle and Turner representation.[24] We used the analytic form of the absorptive scattering factor for the thermal diffuse scattering.[25]

In addition to the thermal diffuse scattering, the absorption due to electronic excitation is also considered. The Fourier component of the absorption potential due to electronic excitation is obtained by

$$V_g^{\text{el}} = -\frac{1}{N}v_0^{\text{el}}\exp(-50s^2)\sum_i \exp(-i\mathbf{g}\cdot\mathbf{R}_i), \quad (8)$$

where N is the number of atoms in a unit cell and v_0^{el} is the mean absorption potential due to electronic excitation.[13] As regards the bulk crystal, the theoretical value of v_0^{el} was determined to be 1.22 V by Radi.[21] Upon substituting Eqs. (3), (6), and (8) into Eq. (2), the total crystal potential can be evaluated.

Figure 3 shows the calculated RHEPD intensity as a function of temperature. In this case, we assumed the atomic coordinates as predicted by the first-principles calculations[12] because the temperature dependence of calculated RHEPD intensities is mostly insensitive to the adatom height. The Debye temperature of the adatoms and the first bilayer (denoted as Θ_S) is maintained at 300 K, and that below the second bilayer (denoted as Θ_B) is changed from 300 to 600 K (see also Table I). The temperature dependences of the (00) and (11) spot intensities at $\theta=1.0°$ for $\Theta_B=300$ K and $\Theta_B=600$ K are nearly the same. Thus, the RHEPD intensity below the critical angle is not affected by the thermal vibration below the second bilayer. The intensity of the (111) Bragg spot is also independent of the bulk property. Therefore, the Debye temperature of the adatoms and the first bilayer can be determined solely under the abovementioned conditions. On the other hand, the temperature dependences of the (444) Bragg reflection intensities are considerably different for $\Theta_B=300$ K and $\Theta_B=600$ K. The intensities of the higher-order Bragg reflections depend mainly on the thermal vibration of the bulk atoms. This is because of the deep penetration of the positrons into the bulk region at high glancing angles. Thus, the Debye temperature below the second bilayer can be determined from the temperature dependences of the intensities of the higher-order Bragg reflections.

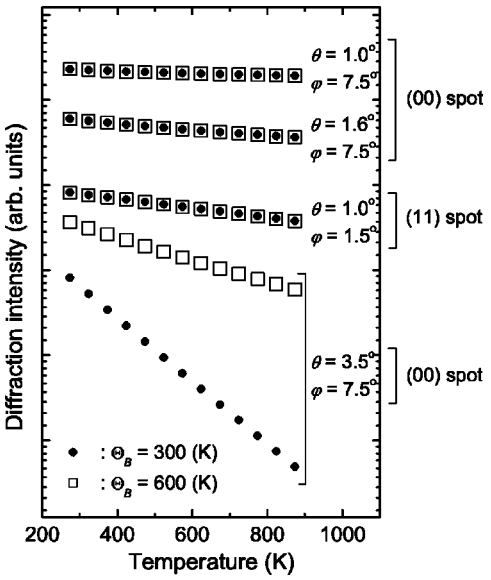

FIG. 3. Temperature dependences of the RHPED intensities from a Si(111)-(7×7) surface obtained from theoretical calculations. The Debye temperature for the adatoms and the first bilayer (Θ_S) was maintained at 300 K and that below the second layer (Θ_B) was varied from 300 K (closed circles) to 600 K (open squares).

To determine the Debye temperature of the surface layer, we varied Θ_S in the calculation so as to reproduce the experimental results. In order to compare the experiments and the theory, the following reliability factor (R) is used:

$$R = \sqrt{\sum_T (I_T^{\text{exp}} - I_T^{\text{cal}})^2}, \quad (9)$$

where $\Sigma_T I_T^{\text{exp}} = \Sigma_T I_T^{\text{cal}} = 100\%$.[25] The minimum R indicates that the slope of the measured intensity is in accordance with the calculated one.

TABLE I. Root mean squares of the thermal vibrational amplitude of the adatoms for the Si(111)-(7×7) surface (unit is angstrom).

Present	X ray[a]	Theory[b]	RHEED[c]
0.14	0.12[d]	0.11[e]	0.09

[a]Reference 25.
[b]Reference 26.
[c]Reference 15.
[d]In plane thermal vibration.
[e]Averaged value over all directions.

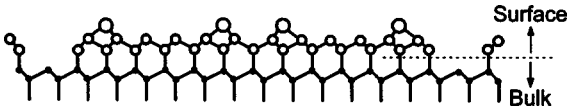

Figure 4(a) shows R as being a function of the Debye temperature, in the case of the (11) spot, which exhibits large temperature dependence. The minimum R is obtained at $\Theta_S = 290$ K. Similarly, from the minimum R for the (444) Bragg spot, $\Theta_B = 600$ K is obtained. The solid lines in Fig. 2 represent the calculated temperature dependences of the diffraction intensities using $\Theta_S = 290$ K and $\Theta_B = 600$ K. The slopes of the calculated intensities are well in accordance with those of the experiments. As mentioned above, the surface Debye temperature can be determined without any influence of the bulk thermal vibration. Consequently, we concluded that the Debye temperature of the topmost surface layer is 290 K, whereas Θ_B is close to the bulk Debye temperature of 505–658 K, as determined by the x-ray diffraction analysis.[1]

We also calculated the RHEPD rocking curves at each temperature using $\Theta_S = 290$ K and $\Theta_B = 600$ K, as obtained above. In a previous study,[8] we found that the profile of the RHEPD rocking curve at a low glancing angle is very sensitive to the adatom height and surface electronic excitation. We used the atomic positions of the adatom height (1.52 Å above the first layer) and the absorption potential (0.25 V) due to the surface electronic excitation determined previously.[8] The absorption potentials due to the surface and bulk electronic excitations do not depend on the temperature. Therefore, these electronic excitations have no influence on the temperature dependence of the RHEPD intensity at the fixed glancing angle (Fig. 3). However, the absorption effect due to the surface and bulk electronic excitations are important in calculations of the RHEPD rocking curves. For example, the surface electronic excitation affects the profile of the curve in the low glancing angle region. In previous study,[8] to a good approximation, we have found that the measured rocking curve can be reproduced by taking into account two absorption potentials due to the surface (0.25 V) and bulk (1.22 V) electronic excitations.

The solid lines in Fig. 1 represent the calculated rocking curves. The calculated curves in the entire temperature range are well in accordance with the experimental curves; that is, the R at each temperature is less than approximately 5%. Thus, the change in a rocking curve with temperature can be explained by the effect of the enhanced thermal vibration amplitude of the surface atoms. The change in the height of the adatoms plays no significant role in the reproduction of the temperature-dependent rocking curve.

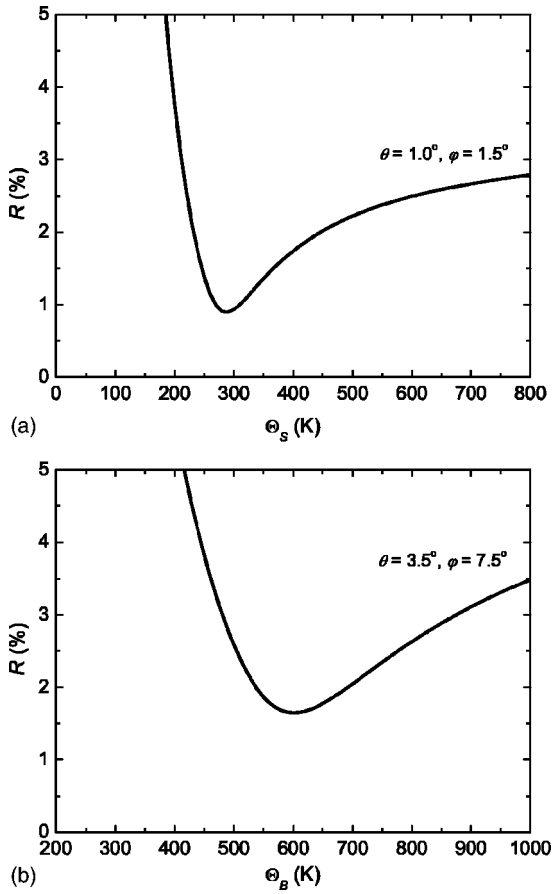

FIG. 4. Reliability factor (R) as a function of the Debye temperature for the first layer (Θ_S), obtained by comparing temperature dependences from the experiment [(11) spot] and the calculations. (b) R as a function of the Debye temperature below the second layer (Θ_B), obtained by comparing temperature dependences from the experiment [(444) Bragg reflection] and the calculations.

Positrons in the total reflection region are diffracted from the topmost surface layer (adatoms and the first layer). Therefore, the topmost surface Debye temperature should be regarded as that of the adatoms. Table I shows the thermal vibrational amplitudes of the adatoms at 293 K, as determined by x-ray diffraction analysis,[26] *ab initio* molecular dynamics calculations,[27] and RHEED.[15] The thermal vibration amplitude of the adatoms obtained in this study is sufficiently large as compared with that obtained by the first-principles calculations[27] and RHEED.[15] This can be compared with the result of the x-ray diffraction analysis with respect to the parallel component of the thermal vibration of the surface.[26] The thermal vibrational amplitude of the adatoms obtained by electron diffraction[15] has clearly been underestimated. It is possible that in electron diffraction, the thermal vibrational amplitude is obtained as an average of the amplitudes between the surface and the bulk. From $\Theta_S = 290$ K, the phonon energy is estimated to be 25 meV. The energy state of the vibrational mode associated with the ada-

toms is actually situated around 25–33 meV and 71 meV, as obtained by the electron energy-loss spectroscopy.[28] Recently, several low vibrational modes localized on the surface layers below 25 meV were located by a large-scale, tight-binding calculation.[17] The existence of the low vibrational modes related to Rayleigh waves is expected to lead to the large vibrational amplitude of the adatoms, particularly at low temperatures. Therefore, the $\Theta_S = 290$ K obtained in this study is considered acceptable as the Debye temperature of the adatoms. The thermal vibrational amplitude of the surface is estimated to be 0.23 Å at 873 K. As a result, the bond of the adatoms becomes soft at a temperature considerably below the 7×7 to 1×1 phase transition temperature (1103 K).

IV. SUMMARY

In summary, we investigated thermal vibration related to the Si(111)-(7×7) surface using RHEPD. We demonstrate that the Debye temperature of the topmost surface can be determined without any influence of the bulk. The thermal vibration amplitude of the adatoms is found to be very large (0.14 Å at 293 K and 0.23 Å at 873 K). These results imply that the bonds of the adatoms become soft.

*Electronic address: fukaya@taka.jaeri.go.jp

[1] *International Tables for X-Ray Crystallography*, Vol. III, edited by C. H. MacGillavry and G. D. Rieck (Kynoch Press, Birmingham, 1968).
[2] A. Ichimiya, Solid State Phenom. **28-29**, 143 (1992).
[3] A. Kawasuso and S. Okada, Phys. Rev. Lett. **81**, 2695 (1998).
[4] A. Kawasuso, K. Kojima, K. Narumi, M. Yoshikawa, and H. Itoh, Appl. Phys. Lett. **76**, 1191 (2000).
[5] A. Kawasuso, M. Yoshikawa, K. Kojima, S. Okada, and A. Ichimiya, Phys. Rev. B **61**, 2102 (2000).
[6] T. Ishimoto, A. Kawasuso, and H. Itoh, Appl. Surf. Sci. **194**, 43 (2002).
[7] A. Kawasuso, T. Ishimoto, S. Okada, H. Itoh, and A. Ichimiya, Appl. Surf. Sci. **194**, 287 (2002).
[8] A. Kawasuso, Y. Fukaya, K. Hayashi, M. Maekawa, S. Okada, and A. Ichimiya, Phys. Rev. B **68**, 241313 (2003).
[9] K. Hayashi, Y. Fukaya, A. Kawasuso, and A. Ichimiya, Appl. Surf. Sci. **237**, 34(2004).
[10] Y. Fukaya, A. Kawasuso, K. Hayashi, and A. Ichimiya, Appl. Surf. Sci. **237**, 29(2004).
[11] K. Takayanagi, Y. Tanishiro, S. Takahashi, and M. Takahashi, Surf. Sci. **164**, 367 (1985).
[12] K. D. Brommer, M. Needels, B. E. Larson, and J. D. Joannopoulos, Phys. Rev. Lett. **68**, 1355 (1992).
[13] A. Ichimiya, Surf. Sci. **192**, L893 (1987).
[14] S. Y. Tong, H. Huang, C. M. Wei, W. E. Packard, F. K. Men, G. Glander, and M. B. Webb, J. Vac. Sci. Technol. A **6**, 615 (1988).
[15] Y. Fukaya, K. Nakamura, and Y. Shigeta, J. Vac. Sci. Technol. A **18**, 968 (2000).
[16] I. K. Robinson and E. Vlieg, Surf. Sci. **261**, 123 (1992).
[17] L. Liu, C. S. Jayanthi, and S.-Y. Wu, Phys. Rev. B **68**, 201301 (2003).
[18] A. Kawasuso, S. Okada, and A. Ichimiya, Nucl. Instrum. Methods Phys. Res. B **171**, 219 (2000).
[19] A. Ichimiya, Jpn. J. Appl. Phys., Part 1 **22**, 176 (1983).
[20] D. M. Bird and Q. A. King, Acta Crystallogr., Sect. A: Found. Crystallogr. **46**, 202 (1990).
[21] G. Radi, Acta Crystallogr., Sect. A: Cryst. Phys., Diffr., Theor. Gen. Crystallogr. **26**, 41 (1970).
[22] Eq. (2.41) in D. P. Woodruff and T. A. Delchar, *Modern Techniques of Surface Science* (Cambridge University Press, Cambridge, 1994). This equation is high temperature limit of Eq. (4).
[23] P. A. Doyle and P. S. Turner, Acta Crystallogr., Sect. A: Cryst. Phys., Diffr., Theor. Gen. Crystallogr. **26**, 390 (1968).
[24] S. L. Dudarev, L.-M. Peng, and M. J. Whelan, Surf. Sci. **330**, 86 (1995).
[25] Y. Fukaya and Y. Shigeta, Phys. Rev. B **65**, 195415 (2002).
[26] I. K. Robinson, W. K. Waskiewicz, P. H. Fuoss, and L. J. Norton, Phys. Rev. B **37**, 4325 (1988).
[27] I. Štich, K. Terakura, and B. E. Larson, Phys. Rev. Lett. **74**, 4491 (1995).
[28] W. Daum, H. Ibach, and J. E. Müller, Phys. Rev. Lett. **59**, 1593 (1987).